

## Turbulence and plasma flow self-organisation in a Reversed Field Pinch configuration

N. Vianello<sup>1</sup>, E. Spada<sup>1</sup>, V. Antoni<sup>1</sup>, M. Spolaore<sup>1</sup>, G. Serianni<sup>1</sup>, G. Regnoli<sup>1</sup>,  
R. Cavazzana<sup>1</sup>, E. Martines<sup>1</sup>, H. Bergsaker<sup>2</sup> and J. R. Drake<sup>2</sup>

<sup>1</sup> *Consorzio RFX, Associazione Euratom-ENEA sulla fusione,  
C.so Stati Uniti 4, I-35127 Padova (Italy)*

<sup>2</sup> *Division of Fusion Plasma Physics (Association Euratom/VR)  
Alfvén Laboratory, Royal Institute of Technology, SE 100 44, Stockholm, Sweden*

Plasma turbulence is a fundamental argument in research for thermonuclear fusion as it is commonly recognised as the dominant mechanism for *anomalous transport* [1]. Since the discovery of improved confinement regimes, the relation between plasma turbulence and sheared plasma flow has become a key subject because of the role played by velocity shear in turbulence suppression [2]. Indeed spontaneous sheared flows due to  $\mathbf{E} \times \mathbf{B}$  drift have been observed in the edge region of tokamaks, stellarators and Reversed Field Pinches (RFP), and in some experiments [3, 4, 5] the value of the spontaneous shear is found marginal for turbulence suppression. This feature has been proposed to underlay a dynamical link between  $\mathbf{E} \times \mathbf{B}$  and turbulent transport which eventually leads to a self-regulation process for turbulence [6]. In this work we address this problem on a Reversed Field Pinch by considering momentum balance equation for a compressible plasma and measuring all the terms involved in flow generation and flow damping. Our model is based on the combination of equation of motion and continuity equation for a compressible plasma:

$$mn \left( \frac{\partial}{\partial t} + \mathbf{V} \cdot \nabla \right) \mathbf{V} = -\nabla p + \mu(\nabla^2 \mathbf{V} + \frac{1}{3} \nabla(\nabla \cdot \mathbf{V})) + \mathbf{J} \times \mathbf{B} + \mathbf{F}^{nf} \quad (1)$$

$$\frac{\partial n}{\partial t} + \nabla \cdot (n\mathbf{V}) = \nabla \cdot \Gamma^0 \quad (2)$$

where  $n$ ,  $p$  and  $\mathbf{V}$  are the plasma density, pressure and velocity,  $m$  is the ion mass,  $\mu$  is the viscosity coefficient,  $\Gamma^0$  is the neutral influx and  $\mathbf{F}^{nf}$  is the neutral friction force estimated according to Ref. [7]. The previous equation may be combined using Ampere's law  $\nabla \times \mathbf{B} = \mu_0 \mathbf{J}$  in the momentum balance equation. We will address only the toroidal component of the momentum balance equation, which represents the direction perpendicular to the main magnetic field at the edge of RFP. In order to understand the role played by fluctuations all the variables involved, i.e. the mass density  $\rho$ ,  $\mathbf{V}$  and  $\mathbf{B}$ , have been divided into mean quantities and fluctuating part

( $\mathbf{V} = \bar{\mathbf{V}} + \tilde{\mathbf{v}}$ ,  $\mathbf{B} = \bar{\mathbf{B}} + \tilde{\mathbf{b}}$ ,  $\rho = \bar{\rho} + \tilde{\rho}$ ). An ensemble average of the toroidal component of the momentum equation has been considered [8], assuming toroidal and poloidal symmetry ( $\frac{\partial}{\partial \phi} = \frac{\partial}{\partial \theta} = 0$ ) for mean quantities and neglecting curvature effects. Also toroidal and poloidal derivatives of the fluctuating components have been neglected compared to the radial ones, as the experimental correlation lengths along these two directions are much longer than that in the radial one. The final expression for the mean momentum then becomes:

$$\begin{aligned} \frac{\partial \langle \rho V_\phi \rangle}{\partial t} + \frac{\partial}{\partial r} \left[ \bar{\rho} \langle \tilde{v}_r \tilde{v}_\phi - \frac{\tilde{b}_r \tilde{b}_\phi}{\bar{\rho} \mu_0} \rangle + \langle \tilde{\rho} \tilde{v}_r \rangle \bar{V}_\phi + \langle \tilde{\rho} \tilde{v}_\phi \rangle \bar{V}_r + \langle \tilde{v}_r \tilde{v}_\phi \tilde{\rho} \rangle \right] = \\ - \frac{\partial}{\partial r} \left( \bar{\rho} \bar{V}_r \bar{V}_\phi - \frac{\bar{B}_r \bar{B}_\phi}{\mu_0} \right) + \mu \frac{\partial^2 \bar{V}_\phi}{\partial r^2} + m \frac{\partial \bar{\Gamma}_r^0}{\partial r} \bar{V}_\phi + \bar{F}_\phi^{nf} \end{aligned} \quad (3)$$

In order to measure all the terms involved in equation (3) a suitable probe which combines electrostatic and magnetic high-bandwidth measurements have been developed.  $\mathbf{E} \times \mathbf{B}$  velocity fluctuations are derived from electric field measurements, where the electric field have been approximated by floating potential gradients while magnetic probes consist of a set of three nested coils which measure the time derivative of the three components of magnetic field. Three of the electrostatic pins are used in triple configuration in order to measure electron density fluctuations. Measurements have been performed in the edge region of Extrap-T2R experiment [9], a medium size RFP ( $R/a = 1.24\text{m}/0.183\text{m}$ ) with molybdenum limiter. The location of the limiter ( $r = 183$  mm) defines a Last Closed Flux Surface (LCFS) and a Scrape Off Layer (SOL) behind it. Data have been collected during the stationary phase of low current ( $\sim 60$  kA) hydrogen discharges. Experimental evidences allow further simplification of equation (3) as  $\bar{B}_r$  vanishes at the edge and all terms containing  $\bar{V}_r$  are found to be negligible. Friction with neutrals results small in the region spanned and previous experiment in T2R [5] and other RFP [4] have shown that in stationary condition the neutral influx  $\Gamma_r^0$  balances electrostatic particle flux  $\Gamma_{es} = \langle \tilde{n} \tilde{v}_r \rangle \approx \Gamma_r^0$ . Equation (3) becomes consequently in stationary condition:

$$\frac{\partial}{\partial r} \left[ \underbrace{\bar{\rho} \langle \tilde{v}_r \tilde{v}_\phi - \frac{\tilde{b}_r \tilde{b}_\phi}{\bar{\rho} \mu_0} \rangle}_A + \underbrace{\langle \tilde{v}_r \tilde{v}_\phi \tilde{\rho} \rangle}_B \right] + \underbrace{m \Gamma_{es} \frac{\partial \bar{V}_\phi}{\partial r}}_C \approx \mu \frac{\partial^2 \bar{V}_\phi}{\partial r^2} \quad (4)$$

The term  $A$  on the left hand side of the previous equation is proportional through

the mass density to the Reynolds stress tensors  $R_{ij} = \langle \tilde{v}_i \tilde{v}_j \rangle - \langle \tilde{b}_i \tilde{b}_j \rangle / \mu_0 \bar{\rho}$ . The term  $B$  represents the three wave coupling between fluctuation of density and of velocities perpendicular to the main magnetic field, whereas the term  $C$  represents the rate of momentum exchange by diffusion in a non-uniform velocity field. In figure 1 we show the various components of terms  $A$  and  $B$  as function of the minor radius together with typical velocity profiles. The two component of Reynolds stress (fig. 1 (c)) have

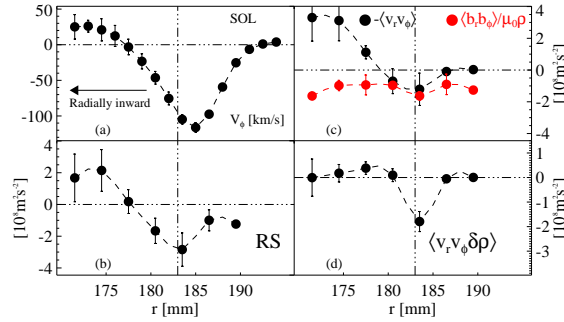


**Figure 1:** (a)  $\mathbf{E} \times \mathbf{B}$  toroidal flow as function of minor radius (b) Complete Reynolds stress tensor (c) Electrostatic and magnetic part of Reynolds stress tensor, (d) triple correlation term (term  $C$  of equation 4) normalised to mean mass density ( $\delta\rho = \frac{\tilde{\rho}}{\bar{\rho}}$ )

comparable order of magnitude but different radial behaviour, as only the electrostatic component exhibits strong radial gradient. Therefore, despite the higher level of magnetic fluctuation observed in a Reversed Field Pinch, the radial gradient of Reynolds stress is mostly due to electrostatic component and is found to take place in the highly sheared region, as observed in stellarators and tokamaks [3, 10]. As shown in figure 1 (d), the term  $B$  (opportunistically normalised to mean mass density) results negligible almost everywhere apart in the region across the LCFS where it is comparable to the Reynolds stress. According to equation 4 the radial derivatives of Reynolds stress and of the triple product, and the term  $C$  oppose the viscous force on the right hand side (RHS) of the same equation. On figure 2(a) the left hand side (LHS) of equation 4 is shown as a function of minor radius. In the same figure the second derivative of  $\mathbf{E} \times \mathbf{B}$  velocity is shown in red dots. As it can be easily seen the two profiles change sign at the same radial position, and they have the same sign at least up to  $r \approx 173$ , where the discrepancy can be attributed to a poor estimate of the derivatives. On figure 2(b) the radial profiles of each of the three summed terms are shown, in order to establish their relative strength and action. Their role depends on the relative sign compared to

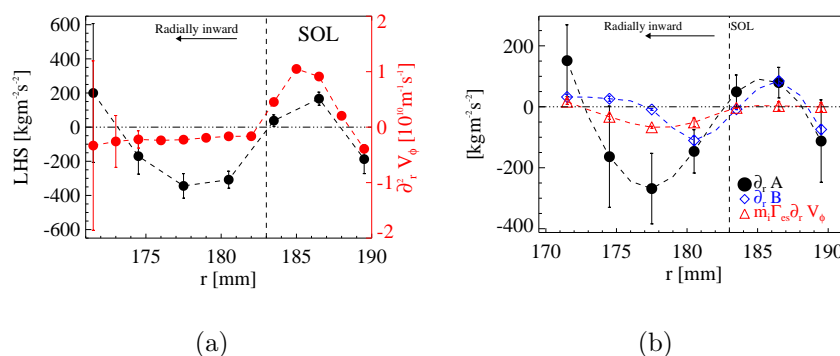


**Figure 2:** (a) Radial profile of LHS of equation 4 and of the second derivative of flow velocity  
(b) Radial profile of the radial derivative of term A of term B and term C

RHS of the equation: terms with the same sign of the second derivative of the velocity are identified as terms opposing the viscous force and viceversa. As it can be easily seen the term proportional to the Reynolds stress is the dominant term inside the LCFS, then manifesting a leading role in flow generation, while the triple correlation term acts in the same way and with the same strength as Reynolds stress in the SOL, whereas for  $r \leq 178$  it gives an additional damp. Therefore, as the viscous force tends to smooth the velocity profile by decreasing its shear, Reynolds stress appears as the term which sustains the shear velocity inside the LCFS. From the rate between the two components shown in figure 2(a) an estimate of perpendicular viscosity may be given, and extending the classical result which links it to diffusivity ( $\mu = \rho D$ ) an effective diffusion coefficient may be derived. The average value is of the order of  $30 \text{ m}^2\text{s}^{-1}$ , at least one order of magnitude greater than classical collisional velocity and of the same order of the effective electrostatic diffusivity estimated from electrostatic particle flux  $D_{el} = \Gamma_{es}/\nabla n_e$ , supporting a turbulence self-regulation process by which mainly Reynolds stress drives the flow against anomalous viscous dissipation.

## References

- [1] B.A.Carreras *et al.*, IEEE Trans.Plasma Science **25** 1281 (1997)
- [2] P.W. Terry, Rev. Mod. Phys. **72**, 109 (2000)
- [3] C. Hidalgo *et al.*, New Journal of Physics **4**, 51.1 (2002)
- [4] V. Antoni *et al.*, Phys. Rev. Lett. **80**, 4185 (1998)
- [5] N.Vianello *et al.*, Plasma Phys. Contr. Fusion **44**, 2513 (2002)
- [6] P.H. Diamond, Y.B. Kim *et al.*, Phys. Fluids B **3**, 1626 (1991)
- [7] M.Tendler and D. Heifetz, Fus. Technology **11**, 289 (1987)
- [8] A.Yoshizawa *et al.*, Plasma Phys. Contr. Fusion **46**, R25 (2004)
- [9] P. Brunzell *et al.*, Plasma Phys. Contr. Fusion **43**, 1457 (2001)
- [10] Y.H.Xu *et al.*, Phys. Rev. Lett. **84**, 3867 (2000)